Journal of Applied Physics

Properties of N-polar AlGaN/GaN heterostructures and field effect transistors grown by metalorganic chemical vapor deposition

Cite as: J. Appl. Phys. **103**, 033708 (2008); https://doi.org/10.1063/1.2838214
Submitted: 15 October 2007 . Accepted: 03 December 2007 . Published Online: 11 February 2008

S. Keller, C. S. Suh, Z. Chen, R. Chu, S. Rajan, N. A. Fichtenbaum, M. Furukawa, S. P. DenBaars, J. S. Speck, and U. K. Mishra

J. Appl. Phys. **103**, 033708 (2008); https://doi.org/10.1063/1.2838214 **103**, 033708

JOURNAL OF APPLIED PHYSICS **103**, 033708 (2008)

Properties of N-polar AlGaN/GaN heterostructures and field effect transistors grown by metalorganic chemical vapor deposition

S. Keller,[a] C. S. Suh, Z. Chen, R. Chu, S. Rajan, N. A. Fichtenbaum, M. Furukawa,
S. P. DenBaars, J. S. Speck, and U. K. Mishra
Electrical and Computer Engineering Department, University of California, Santa Barbara, California 93106, USA and Materials Department, University of California, Santa Barbara, California 93106, USA

(Received 15 October 2007; accepted 3 December 2007; published online 11 February 2008)

Smooth N-polar GaN/$Al_xGa_{1-x}N$/GaN heterostructures with a different Al mole fraction were grown by metalorganic chemical vapor deposition on (0001) sapphire substrates with a misorientation angle of 4° toward the *a*-sapphire plane. The sheet electron density of the two-dimensional electron gas (2DEG), which formed at the upper GaN/$Al_xGa_{1-x}N$ interface increased with an increasing Al-mole fraction in the $Al_xGa_{1-x}N$ layer and increasing silicon modulation doping, similar to the observations for Ga-polar heterostructures. The transport properties of the 2DEG, however, were anisotropic. The growth on vicinal substrates led to the formation of well ordered multiatomic steps during $Al_xGa_{1-x}N$ growth and the sheet resistance of the 2DEG parallel to the steps was about 25% lower than the resistance measured in the perpendicular direction. The fabricated devices exhibited a drain-source current, I_{DS}, of 0.9 A/mm at a gate-source voltage +1 V. At a drain-source voltage of 10 V and $I_{DS}=300$ mA/mm, current-gain and maximum oscillation frequencies of 15 and 38 GHz, respectively, were measured.
[DOI: 10.1063/1.2838214]

I. INTRODUCTION

While today's Ga-polar GaN based field effect transistors (FETs) show excellent performance for high power and high frequency applications as well as for power switching, N-polar device structures have been much less investigated. The opposite direction of the piezoelectric and spontaneous polarization field in N-polar GaN/AlGaN heterostructures was verified already in early experiments, revealing their potential for future device applications.[1,2] N-polar heterostructures are particularly attractive for highly scaled transistors, enhancement mode transistors, and sensor applications. The exploration of N-polar (Al,Ga)N heterostructures and devices was, however, hampered by difficulties in their growth, as N-polar GaN films often exhibited hexagonal hillocks leading to rough surfaces.[3] More recently, smooth N-polar AlGaN/GaN heterostructures and devices were demonstrated by molecular beam epitaxy (MBE) using C-polar SiC as the substrate.[4–6] Here we report on the growth of N-polar GaN/AlGaN heterostructures and FETs by metalorganic chemical vapor deposition (MOCVD). In this study we investigated the properties of GaN/$Al_xGa_{1-x}N$/GaN heterostructures with a different Al mole fraction and Si doping in the barrier layer and fabricated devices from selected wafers.

II. EXPERIMENT

All samples were grown by low-pressure MOCVD using trimethylgallium (TMGa), trimethylaluminum (TMAl), and ammonia as precursors. (0001) sapphire with a misorientation angle of 4° toward the *a*-sapphire plane was used as the substrate to enable the growth of smooth films.[7] Prior to GaN deposition, the sapphire substrates were annealed in H_2 for 20 min at 1220 °C. Afterwards the temperature was lowered to 1100 °C and 90 mmol/min NH_3 were injected for 2 min to nitridize the sapphire substrate. The GaN deposition was initiated with the growth of a 20 nm thick GaN layer with a TMGa flow, f_{TMGa}, of 11 μmol/min, and an NH_3 flow, f_{NH_3}, of 90 mmol/min at 1050 °C. Afterwards a 1.35 μm thick GaN layer was grown with $f_{TMGa}=85$ μmol/min and $f_{NH_3}=20$ mmol/min at 1200 °C. Simultaneously, 40 nmol/min of bis-cyclopentadienyl-iron were injected to compensate for the enhanced incorporation of oxygen impurities, which act as electron donors, in the initial stage of GaN growth on sapphire. This procedure is similar to those previously reported for the growth of semi-insulating (S.I.) Ga-polar GaN films on sapphire.[8] On top of the Fe-doped layer, a 0.15 μm thick unintentionally doped (uid) spacer layer was deposited with $f_{TMGa}=56$ μmol/min and $f_{NH_3}=160$ mmol/min to separate the Fe-doped base and the active region of the device structure. Afterwards, the growth temperature was lowered to 1145 °C for the deposition of a 17–23 nm thick Si doped $Al_xGa_{1-x}N$ layer using TMGa flows between 6.8 and 8.5 μmol/min, TMAl flows between 3 and 5 μmol/min, and disilane flows between 0 and 0.7 nmol/min, followed by a 6 to 7 nm thick uid $Al_xGa_{1-x}N$ layer of the same composition. The structures were finished with the deposition of the 30 nm thick uid GaN cap layer using $f_{TMGa}=8.5$ μmol/min and $f_{NH_3}=140$ mmol/min. The reactor pressure was kept constant at 100 Torr. A schematic of the sample structure and the band diagram is illustrated in Fig. 1. To evaluate the surface/interface properties, additional samples were fabricated, where the growth was stopped after the deposition of the uid $Al_xGa_{1-x}N$ layer. The $Al_xGa_{1-x}N$ layer growth rate and composition were determined from

---

[a] Electronic mail: stacia@ece.ucsb.edu.

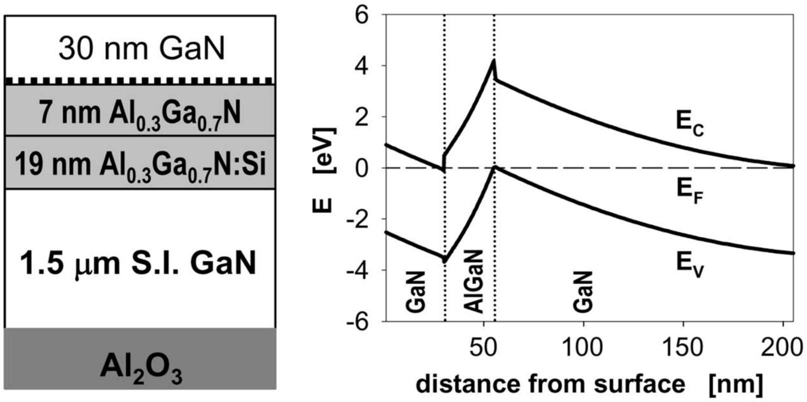

FIG. 1. Schematic of the sample structure and the band diagram.

analysis of x-ray diffraction (XRD) $\omega-2\theta$ scans across the (0004) reflection of 7 period $Al_xGa_{1-x}N/GaN$ multiquantum well (MQW) calibration structures grown under the same conditions.[9] In addition, the quality of the N-polar GaN base layers was evaluated using GaN:Si/S.I. GaN metal–semiconductor FET (MESFET) structures.

Atomic force microscopy (AFM) images were taken with a Digital Instruments Dimension 3100 instrument, operated in tapping mode. The root-mean-square (rms) surface roughness was calculated using the AFM software. The XRD measurements were recorded with a Philips materials research diffractometer. The electrical properties of the two-dimensional electron gas (2DEG), which formed at the upper GaN/AlGaN interface, were evaluated by Van der Pauw–Hall measurements and transfer length method (TLM) measurements. Capacitance-voltage $(C-V)$ measurements were performed at a frequency of 1 MHz using circular test patterns with a diameter of 170 μm. Devices with a gate length of 0.7 μm, a source to gate spacing of 0.7 μm, and a gate to drain spacing of 2.0 μm were fabricated. The gate width was 2×75 μm. A Ti/Al/Ni/Au (20/100/10/50 nm) source and drain ohmic metal stack was deposited by electron (e)-beam evaporation and subsequently subjected to a 30 s rapid thermal annealing at 870 °C in a N_2 atmosphere for 30 s. A Cl_2-based dry etch was used for mesa isolation. A Ni/Au (30/250 nm) gate metal stack was e-beam deposited and the sample was passivated with a 160 nm thick silicon nitride layer grown by plasma-enhanced chemical vapor deposition. The current-voltage $(I-V)$ characteristic of the devices was measured using an Agilent 4154 semiconductor parameter analyzer. Small-signal high frequency measurements were carried out using on-wafer probes and an Agilent 8263a network analyzer.

III. RESULTS AND DISCUSSION

The high quality of the S.I. N-polar GaN base layers grown using the procedure described earlier was reflected in the properties of the MESFET test structures. For electron concentrations of 9×10^{16} cm^3 and 1×10^{18} cm^3, the measured electron mobility values were 650 and 370 cm^2/V s, respectively, which are comparable to Ga-polar samples. The $\omega-2\theta$ scan across the (0004) reflection recorded for one of the MQW calibration samples is displayed in Fig. 2 together with the simulated data.[9] Distinct MQW related higher order satellite peaks and Pendellösung fringes indicated good periodicity and a high quality of the MQW.

The results of the Hall measurements performed on $GaN/Al_xGa_{1-x}N/GaN$ samples with a different Al mole fraction, x_{Al}, in the $Al_xGa_{1-x}N$ layer and grown with a constant disilane flow of 0.25 nmol/min resulting in a Si doping concentration of $\sim 2\times 10^{18}$ cm^{-3} in the $Al_xGa_{1-x}N:Si$ layer are plotted in Fig. 3. The modulation doping was introduced to enhance the stability of the 2DEG charge at the upper GaN/AlGaN interface.[6] As expected, the sheet electron density, n_s, steadily increased with increasing x_{Al} from 1×10^{13} cm^{-2} ($x_{Al}=0.2$) to 1.8×10^{13} cm^{-2} ($x_{Al}=0.36$), while the electron mobility, μ, decreased from 900 to 740 cm^2/V s, except for the sample with the lowest Al mole fraction of 0.2, for which a value of 735 cm^2/V s was measured. Lower mobility values than expected were previously measured also for Ga-polar AlGaN/GaN heterostructures with $x_{Al}\leq 0.2$ and were associated with a reduced screening of interface states at low x_{Al}.[10] While the N-polar samples followed the general trends observed for Ga-polar samples, the sheet electron density

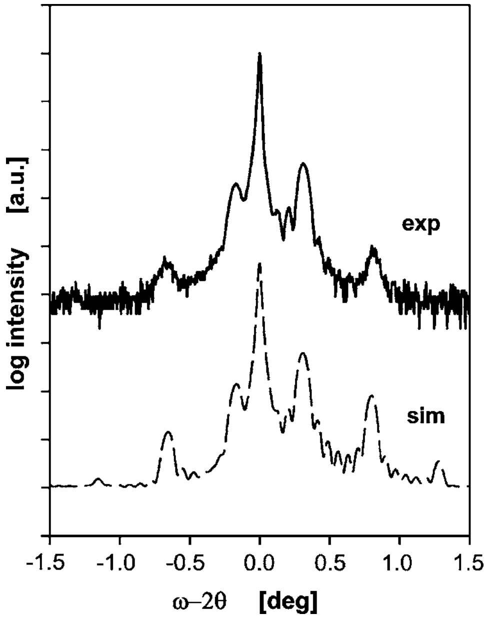

FIG. 2. (0004) reflection $\omega-2\theta$ XRD scan recorded for a 7 period N-polar (6 nm $Al_{0.27}Ga_{0.63}N$/5.3 nm GaN) MQW sample (solid line) and corresponding simulation using dynamic diffraction theory (dashed line).

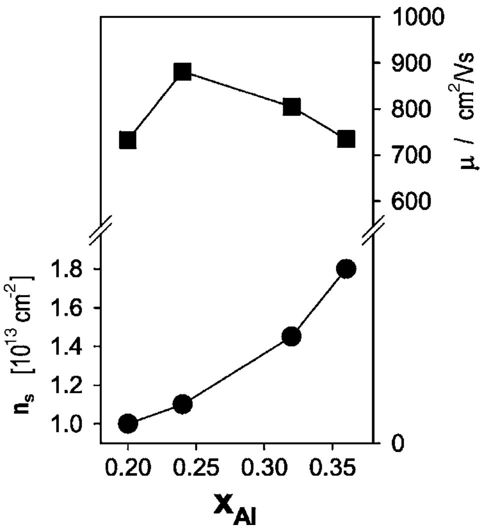

FIG. 3. Dependence of the sheet electron concentration (circles) and the electron mobility (squares) determined by Van der Pauw–Hall measurements at 300 K on the Al mole fraction in the Al$_x$Ga$_{1-x}$N layer.

was somewhat higher and the electron mobility lower. The higher n_s values were most likely caused by the higher residual oxygen concentrations in N-polar in comparison to Ga-polar GaN films,[11] which under the cap layer growth conditions were below the detection limit of 2×10^{16} cm^{-3} in secondary ion mass spectroscopy measurements for Ga-polar films in comparison to 1×10^{17} cm^{-3} for N-polar GaN layers. A higher oxygen content was expected for the Al containing layers.[12]

To gain further understanding of the processes limiting the electron mobility of the 2DEG forming at the upper GaN/Al$_x$Ga$_{1-x}$N interface of the N-polar heterostructures, additional samples with $0.2\leq x_{\mathrm{Al}}\leq0.36$ were fabricated, where the growth was stopped prior to the deposition of the GaN cap layer, and the surface morphology was studied by AFM. As seen in the image taken from the Al$_{0.32}$Ga$_{0.68}$N/S.I. GaN sample (Fig. 4), the sample surface was characterized by a high density of steps parallel to the $\langle 11\bar{2}0\rangle_{\mathrm{GaN}}$ direction caused by misorientation of the (Al,Ga)N crystal, which in turn originated from the substrate misorientation.[7] Note that the average terrace width seen in the AFM image (~16 nm) was significantly larger than the width expected for steps with a height of 0.26 nm as seen on Ga-polar GaN,[13] which would result in a terrace width of 3.7 nm on 4° misoriented substrates, far beyond the lateral resolution of the AFM instrument. This observation implied the formation of multiatomic steps with an estimated overall height of about 2 unit cells.[14] The rms values derived from the AFM images of the samples were between 0.5 and 0.6 nm for 5×5 μm^2 scans. The surface roughness was little affected by the Al mole fraction in the AlGaN layer.

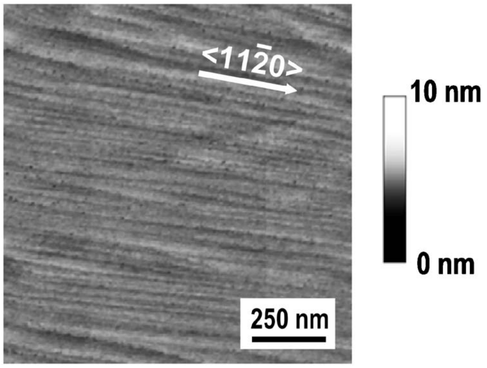

FIG. 4. Atomic force microscopy image of a 26 nm thick Al$_{0.32}$Ga$_{0.68}$N grown on top of 1.5 μm S.I. GaN.

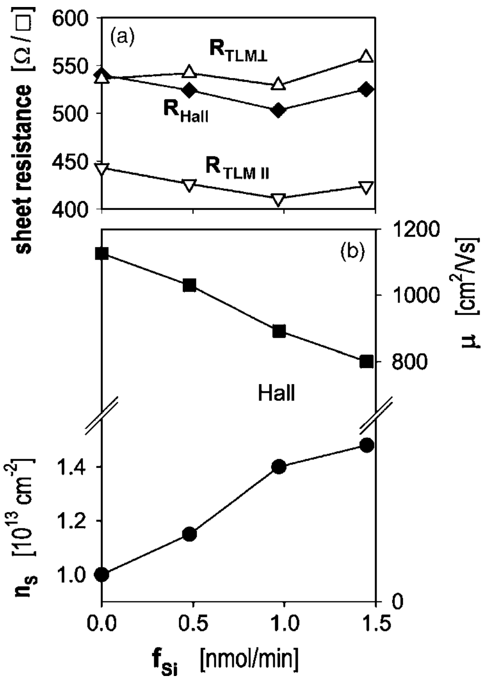

FIG. 5. (a) Dependence of sheet resistance of the 2DEG measured at 300 K using TLM patterns parallel (triangles down) and perpendicular (triangles up) to the step direction and derived form the Van der Pauw–Hall measurements (diamonds) on the silicon doping in the Al$_{0.28}$Ga$_{0.62}$N:Si layer. (b) Dependence of the sheet electron concentration (circles) and the electron mobility (squares) determined by Van der Pauw–Hall measurements at 300 K on the silicon doping in the Al$_{0.28}$Ga$_{0.62}$N:Si layer.

To explore the influence of the multiatomic steps at the GaN/Al$_x$Ga$_{1-x}$N interface on the properties of the 2DEG, the second series of samples with different Si doping was not only evaluated using Van der Pauw–Hall measurements, but also by TLM measurements using patterns parallel and perpendicular to the step direction. The layer structure was comprised of a 19 nm Al$_{0.28}$Ga$_{0.62}$N:Si layer with different doping and a 7 nm thick uid Al$_{0.28}$Ga$_{0.62}$N spacer layer. In addition, the switching time between the uid AlGaN spacer layer and the GaN cap layer was increased to 4 s, in comparison to 2 s used for the samples of the Al composition series. The results of the Van der Pauw–Hall measurements are plotted in Fig. 5(b). With increasing Si doping, n_s increased from 1×10^{13} cm^{-2} for the undoped sample to 1.48×10^{13} cm^{-2} for the sample grown with a disilane flow of 0.7 nmol/min. Simultaneously, the mobility of the 2DEG decreased from 1110 to 800 cm^2/V s. The decrease of the electron mobility with increasing n_s was expected as the higher the sheet electron density, the more closely the electrons are pushed toward the interface, and the more the electron transport is affected by the interface roughness and alloy scattering.[15] The measured electron mobility values for this

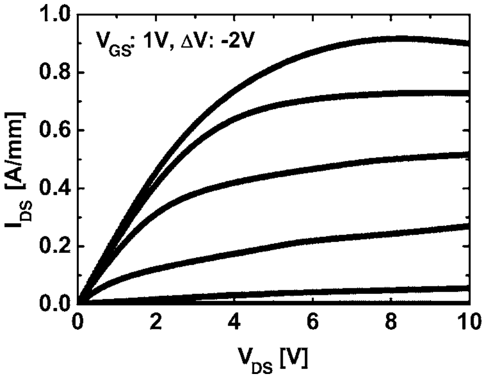

FIG. 6. $I-V$ characteristic of a transistor fabricated from the 30 nm GaN/26 nm $Al_{0.28}Ga_{0.62}N$/S.I. GaN wafer.

series of samples were generally somewhat higher than those of the Al composition series, possibly related to a more abrupt compositional change at the $GaN/Al_{0.28}Ga_{0.62}N$ interface caused by the longer switching time of 4 s used during growth. The sheet resistance of the 2DEG derived from Hall and TLM measurement for patterns oriented parallel and perpendicular to the interface steps are illustrated in Fig. 5(a), revealing a strong anisotropy of the electron transport. The sheet resistance measured parallel to the interface steps was generally much lower (400–450 $\Omega/\square$) compared to the resistance measured perpendicular to the steps (530–600 $\Omega/\square$). Note that the n_s values derived from $C-V$ measurements also performed on the samples were within the 5% margin of the n_s values determined from the Hall measurements. A strong anisotropy in the 2DEG properties was previously observed for Ga-polar AlGaN/GaN structures grown on vicinal substrates and associated with an enhanced electron mobility parallel to the steps at the AlGaN/GaN interface due to reduced interface roughness.[16,17] Assuming that the differences in the sheet resistance are related exclusively to differences in the electron mobility of the 2DEG parallel and perpendicular to steps, for the undoped $GaN/Al_{0.28}Ga_{0.62}N/GaN$ sample an electron mobility value as high as 1400 $cm^2/V\,s$ can be calculated from n_s and the TLM sheet resistance parallel to the step direction, in comparison to 1160 $cm^2/V\,s$ in the perpendicular direction. Further investigations are presently under way to gain a deeper understanding of the anisotropic properties of the 2DEG observed for the N-polar heterostructures in this study.

The $I-V$ characteristic of a transistor fabricated from the undoped sample is shown in Fig. 6. The source and drain contacts were aligned in such a way, that the electron transport in the device occurred parallel to the direction of the steps at the $GaN/Al_{0.28}Ga_{0.62}N$ interface. The contact resistance was 0.4 Ω mm. At a gate-source voltage, V_{GS}, of +1 V, the drain-source current, I_{DS}, was 0.9 A/mm and the threshold voltage was approximately −7.5 V. At a drain-source voltage, V_{DS}, of 10 V and $I_{DS}=300$ mA/mm, the device exhibited a peak current-gain cutoff frequency, f_T, of 15 GHz and a peak maximum oscillation frequency, f_{max}, of 38 GHz. These results are in the range of those reported for basic Ga-polar AlGaN/GaN FETs (Ref. 18) and MBE grown N-polar GaN/AlGaN devices with similar device dimensions.[6] Improvements in the device performance are expected through further optimization of the growth process and implementation of an AlN spacer layer (device structure: $GaN/AlN/Al_xGa_{1-x}N$/S.I. GaN), mitigating alloy scattering at the $GaN/Al_xGa_{1-x}N$ interface.[19]

IV. CONCLUSIONS

In conclusion, N-polar $GaN/Al_xGa_{1-x}N/GaN$ structures with electron sheet carrier concentrations and electron mobilities comparable to Ga-polar $Al_xGa_{1-x}N/GaN$ heterostructures were fabricated by MOCVD on vicinal sapphire substrates. The use of vicinal substrates, however, led to anisotropy in the properties of the 2DEG, reflected in a 25% lower sheet resistance of the 2DEG for conduction parallel to the step direction in comparison to the perpendicular one. Finally, initial FETs exhibited promising results with drain-source currents of 0.9 A/mm and f_T and f_{max} values of 15 and 38 GHz, respectively.

ACKNOWLEDGMENTS

The authors gratefully acknowledge the support of the USAFOSR (Dr. K. Reinhardt and Dr. J. Witt) and the ONR-MINE program (Dr. Paul Maki and Dr. Harry Dietrich).

[1] R. Dimitrov, M. Murphy, J. Smart, W. Schaff, J. R. Shealy, L. F. Eastman, O. Ambacher, and M. Stutzmann, J. Appl. Phys. **87**, 3375 (2000).
[2] F. Bernardini, V. Fiorentini, and D. Vanderbilt, Phys. Rev. B **56**, R10024 (1997).
[3] M. Sumiya, K. Yoshimura, T. Ito, K. Ohtsuka, S. Fuke, K. Mizuno, M. Oshimoto, H. Koinuma, A. Ohtomo, and M. Kawasaki, J. Appl. Phys. **88**, 1158 (2000).
[4] E. Monroy, E. Sarigiannidou, F. Fossard, N. Gogneau, E. Bellet-Amalric, and J. L. Rouviere, Appl. Phys. Lett. **84**, 3684 (2004).
[5] S. Rajan, M. Wong, Y. Fu, F. Wu, J. S. Speck, and U. K. Mishra, Jpn. J. Appl. Phys., Part 2 **44**, L1478 (2005).
[6] S. Rajan, A. Chini, M. H. Wong, J. S. Speck, and U. K. Mishra, J. Appl. Phys. **102**, 044501 (2007).
[7] S. Keller, N. A. Fichtenbaum, F. Wu, D. Brown, A. Rosales, S. P. DenBaars, J. S. Speck, and U. K. Mishra, J. Appl. Phys. **102**, 083546 (2007).
[8] S. Heikman, S. Keller, S. P. DenBaars, and U. K. Mishra, Appl. Phys. Lett. **81**, 439 (2002).
[9] O. Brandt, P. Waltereit, and K. H. Ploog, J. Phys. D **35**, 577 (2002).
[10] S. Keller, G. Parish, P. T. Fini, S. Heikman, C. H. Chen, N. Zhang, S. P. DenBaars, and U. K. Mishra, J. Appl. Phys. **86**, 5850 (1999).
[11] M. Sumiya, K. Yoshimura, K. Ohtsuka, and S. Fuke, Appl. Phys. Lett. **76**, 2098 (2000).
[12] G. Parish, S. Keller, S. P. DenBaars, and U. K. Mishra, J. Electron. Mater. **29**, 15 (2000).
[13] D. Kapolnek, X. H. Wu, B. Heying, S. Keller, B. P. Keller, U. K. Mishra, S. P. DenBaars, and J. S. Speck, Appl. Phys. Lett. **67**, 1541 (1995).
[14] J. Ishizaki, S. Goto, M. Kishida, T. Fukui, and H. Hasegawa, Jpn. J. Appl. Phys., Part 1 **33**, 721 (1994).
[15] Y. Zhang and J. Singh, J. Appl. Phys. **85**, 587 (1999).
[16] X. Q. Shen, H. Okumura, K. Furuta, and N. Nakamura, Appl. Phys. Lett. **89**, 171906 (2006).
[17] N. Nakamura, K. Furuta, X. Q. Shen, T. Kitamura, K. Nakamura, and H. Okumura, J. Cryst. Growth **301–302**, 452 (2007).
[18] K. Kunihiro, K. Kasahara, Y. Takahashi, and Y. Ohno, Jpn. J. Appl. Phys., Part 1 **39**, 2431 (2000).
[19] L. Shen, S. Heikman, B. Moran, R. Coffie, N. Q. Zhang, D. Buttari, I. P. Smorchkova, S. Keller, S. P. DenBaars, and U. K. Mishra, IEEE Electron Device Lett. **22**, 457 (2001).